CCN predictions on particles containing mixed organic and elemental carbon using Köhler theory

Jessie Creamean[1†] et al.
[1]University of California, San Diego, La Jolla, California

Anthropogenic atmospheric aerosols play a large role in climate change by acting as cloud condensation nuclei (CCN) and influencing cloud reflectivity. The ability of anthropogenic aerosols to contribute to cloud droplet activation depends on particle size and composition. Up to 90% of fine particle mass ($PM_{2.5}$) is composed of carbonaceous (elemental and organic carbon) compounds, which play a significant yet unknown role in cloud droplet activation. While elemental carbon (EC) has limited solubility and mainly contributes to particle size, the organic carbon (OC) could add a substantial amount of soluble material to the particle depending on the nature of the organic species present. Here we present size-resolved aerosol measurements of single-particle chemistry in an urban environment that was heavily influenced by carbonaceous particle types (OC and EC particles accounted for 43.5% and 39.1% of the total submicron particle count, respectively). Köhler calculations were used to determine the CCN activity of different particle diameters of internally mixed OC and EC particles. Our results demonstrate how the soluble fraction (%OC) and size of observed mixed OC and EC-containing particles affect the ability to act as CCN and how sensitivity parameters such as density, solubility, and molecular weight impact CCN. Compared to pure 600 nm EC-containing particles, adding 40% OC (using oxalic acid parameters) to the particles decreased the critical supersaturation from 0.28% to 0.021% and increased the fraction of CCN from 0.264 to 0.815. This means that organic compounds could contribute significantly to cloud droplet number concentration and potentially to the Twomey effect in highly aged urban environments.

1. Introduction

Although tropospheric aerosols contribute to atmospheric cooling, they are the least understood factor in radiative forcing estimates (Solomon and Marquis, 2007). Aerosols that act as cloud condensation nuclei (CCN) to form new cloud droplets usually contain hygroscopic components and are within the size range of 0.1-1.0 μm.

Carbonaceous particles from fossil fuel combustion can constitute a large fraction of tropospheric aerosols (Koch, 2001), especially in urban regions. These particle types include elemental carbon (EC), organic carbon (OC), or a mixture of both. EC particles are characterized by carbon clusters and OC particles may contain carbon, hydrogen, oxygen, sulfur, and nitrogen components. OC can be hygroscopic (Novakov and Penner, 1993), meaning that mixed EC and OC-containing particles may act as CCN depending on the mixing state and size.

Riverside, California represents an aged urban environment that experiences high levels of particulate EC and OC. Due to the aged nature of Riverside, we predict that OC has undergone atmospheric processing and therefore is considered soluble. Here, we use single-particle measurements from the aerosol time-of-flight mass spectrometer (ATOFMS) during the Study of Organic Aerosols in Riverside (SOAR-I) to predict the CCN activity of mixed EC/OC particles at different sizes using a Köhler calculation. Details on ATOFMS and SOAR-I are described elsewhere (Gard et al., 1997; Qin et al., *In preparation.*). OC and EC particles accounted for 43.5% and 39.1% of the total submicron particle count, respectively. The mixing states are not constant with size; therefore, both size and chemical composition play a role in our modeled predictions. The dominant effect must be determined by model calculations. We hypothesize that the critical supersaturation (S_c) will be lower with an increase in the OC solubility of the particle.

2. Köhler Model for Calculating CCN

Particle size and chemical composition of EC and OC acquired from the ATOFMS (Gard et al., 1997) were used as model inputs to calculate the S_c and number of CCN cm^{-3} using the Köhler model from Roberts et al. (2002). The model calculates equilibrium saturation ratio (S_v^{eq}) of a droplet of a given diameter (D_p) and temperature (T) described by a multi-component Köhler equation as

$$S_v^{eq} = \exp\left(\frac{4\sigma' M_w}{kT\rho_w D_p} - \frac{\Phi M_w}{\frac{\pi\rho' D_p^3}{6} - \sum_i m_i} \left[\sum_i \frac{v_i m_i}{M_i} \right] \right) \quad (1)$$

†This work was completed by Jessie Creamean as part of SIO217D term projects advised by Lynn Russell from experimental measurements by Kerri Pratt, Andrew Ault, Xueying Qin, Cassandra Gaston, and Laura Shields as part of a research project developed by Kimberly Prather. Models for this project were developed by Greg Roberts and technical and writing help was provided by Doug Day, non-anonymous, and anonymous reviewers. However, the submitted work has not yet been reviewed and approved by all of the coauthors and is not suitable for citation at this stage. Please contact jcreamean@ucsd.edu to receive an update on these results.

where k is the Boltzmann constant, σ' is the surface tension of the solution, M_w and M_i are the respective molecular weights of water and solute, m_i is the dissolved solute mass, ρ_w and ρ^o are the densities of water and aqueous solution, respectively, υ_i is the van't Hoff factor, and Φ is the osmotic coefficient of the aqueous solution. The maximum S_v^{eq} defines S_c. Figure 1 shows the submicron size distributions of the EC and OC particle types with medians at 550 nm and 700 nm, respectively (range = 200-1000 nm). The fraction of OC particles to total carbon (EC + OC particles) at a particular size was assumed to be the soluble fraction. Different values of S_c were calculated by assuming the OC was the soluble component of the particles. Particles were also assumed to be spherical.

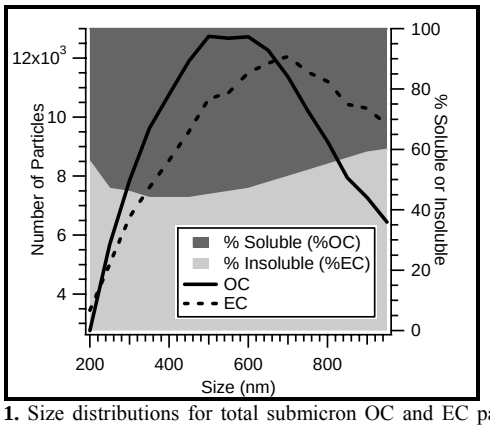

Figure 1. Size distributions for total submicron OC and EC particles during SOAR-1. The dark grey shading represents the soluble fraction (%OC) for each respective size and the light grey represents the insoluble fraction (%EC).

Physical characteristics for EC and OC used as input parameters in the model are shown in Table 1. EC characteristics were determined from Spencer and Prather (2006), while OC characteristics were determined by assuming OC is equivalent to oxalic, glutaric, or pinonic acids (Cruz and Pandis, 2000; Kuwata et al., 2008; Spencer and Prather, 2006). Oxalic acid is the predominantly used substitute for OC due to its high contribution to urban environments (Kuwata et al., 2008). Glutaric acid represents a major component of the water-soluble primary and secondary OC mass in the atmosphere, from the oxidation of cyclic olefins by ozone (Grosjean and Friedlander, 1975). Pinonic acid is an oxidation product of α-pinene (Yokouchi and Ambe, 1985). Because both acids have been previously studied and are abundant in the atmosphere (Cruz and Pandis, 2000), they were chosen as proxies for the OC fraction in addition to oxalic acid in this study.

Once S_c for the various sizes and soluble fractions were determined, the concentration of CCN cm^{-3} was calculated using mean diameters from the 2 median sizes (550 nm and 700 nm) with corresponding soluble fractions for each of those sizes. OC was again assumed to be equivalent to oxalic, pinonic, or glutaric acid.

Table 1. Model input parameters for EC and for assumptions of oxalic, glutaric, or pinonic acids being representative of OC. Types represent respective acid mixed with EC.

Component	Type	ρ (g/mL)	Solubility (g/mL)	MW (g/mol)
EC	n/a	1.887	0	12
Oxalic	1	1.9	0.143	90
Glutaric	2	1.424	1.16	132
Pinonic	3	0.786	0.006	184

3. Predicted S_c and CCN of Mixed Carbonaceous Particles from Model

A mixed EC and OC particle type was modeled using physical characteristics of oxalic acid (see Table 1). Figure 2 shows the calculated S_c from holding size or soluble fraction constant of this mixed particle type, herein called Type 1. Each particle size contains a different mixing state of OC and EC (Figure 1), and therefore, a different percentage of soluble fractions ranging from 40-56%. The effects of size versus soluble fraction on S_c were compared by holding size or soluble fraction constant (Figure 2). The soluble fraction of the mixed particle was varied from 10-90% to show the effect of OC as a solute over a larger range than the ambient measurements.

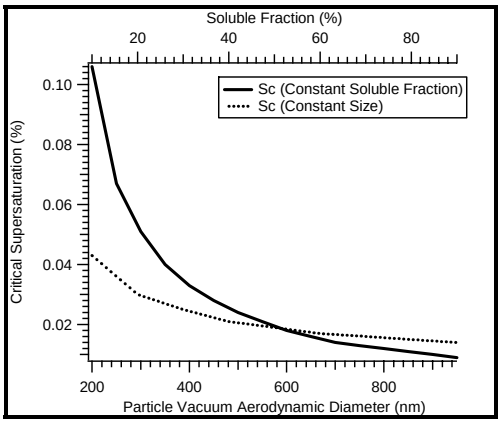

Figure 2. Critical supersaturations of constant size (600 nm) with varying observed solubility fractions (dashed line) and of constant solubility fraction (56% soluble) with varying observed particle sizes (solid line) for mixed OC and EC Type 1 particles.

As the vacuum aerodynamic diameter (D_{va}) of the particle increases when holding the soluble fraction constant (56%), the S_c decreases exponentially. However, as the soluble fraction increases holding size constant (600 nm), the S_c roughly decreases more linearly. To assess the magnitude of the Kelvin and Raoult effects on the different S_c calculated in Figure 2, the standard deviation (σ) of the S_c at constant soluble fraction (σ = 0.026%) was compared to the σ of S_c for the solubility fractions at constant particle size (σ = 0.009%). The constant soluble fraction (56%) was chosen because it was the most common among the different sizes and the constant size (600 nm) was chosen because it was the median of the entire size range (200-1000 nm).

Sensitivity analysis was conducted on the model, using different chemical characteristics for OC. The characteristics used for Type 1 and also the mixed EC and OC particle Types 2 and 3 are described in Table 1. Figure 3 shows the modeled size-resolved profiles of S_c using the different particle types with soluble fractions ranging from 40-56%. Also included for comparison are model results for pure EC and pure OC particles, although these pure types were not observed during ambient measurements.

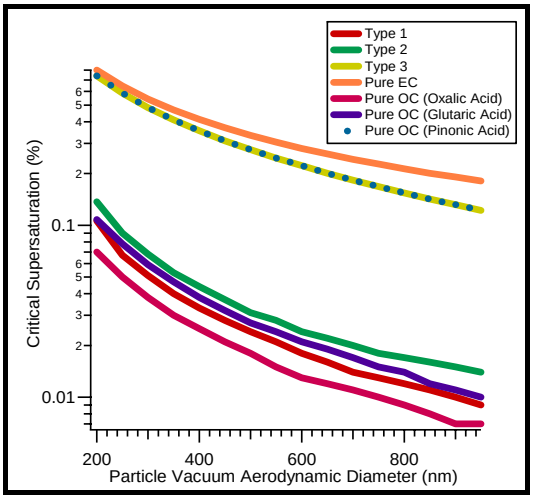

Figure 3. Model calculations of S_c at different particle diameters with different acids used for OC. Also shown are calculations of pure EC and pure OC. Note that Type 3 and Pure OC (Oxalic acid) overlap.

The CCN concentrations were calculated by using the soluble fractions present at the size modes as 550 nm and 700 nm for each particle type (EC and OC, respectively) to determine the number of active particles at different supersaturations. The 550 nm mode contained 54% soluble OC (as Type 1) and the 700 nm mode contained 49% soluble OC. Both modes were assumed to contain 1000 particles cm^{-3}. Figure 4 shows the number concentrations of CCN as the supersaturation is increased. Pictured is the mode at 550 nm only; the 700 nm mode had similar curves, but shifted to the left (lower S_c). Compared to pure EC-containing particles, adding 40% OC (using oxalic acid parameters) to the particles decreased the critical supersaturation from 0.28% to 0.021% and increased the CCN from 264 cm^{-3} to 815 cm^{-3} out of a total 1000 particles cm^{-3}. When comparing the different Types at ~0.02 % supersaturation, Types 1, 2, and 3 attained CCN concentrations of 815 cm^{-3}, 736 cm^{-3}, and 243 cm^{-3}, respectively.

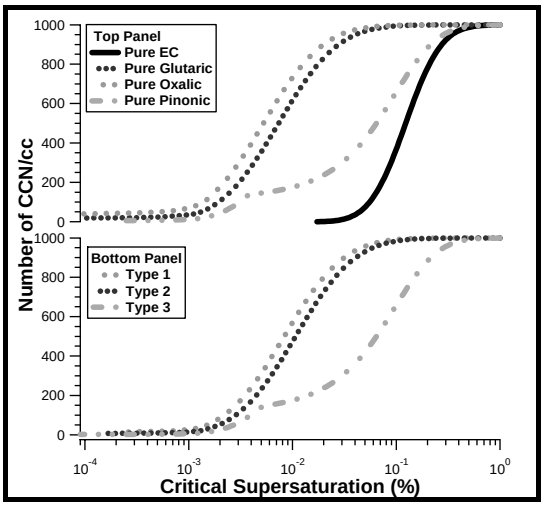

Figure 4. Model calculations of the number concentrations of CCN cm^{-3} at specific S_c for the 550 nm mode. The top panel contains curves for pure EC and OC (as oxalic, glutaric, or pinonic acids) and the bottom panel contains curves for mixtures of EC with oxalic, glutaric, or pinonic acids.

4. Discussion

In Figure 2, it is observed that the effect of solubility does not impact S_c as much as size, which is explained by the standard deviations (σ) of S_c at constant solubility and constant size. The σ of S_c at constant solubility is much larger than σ of the different solubility fractions at one size, suggesting the dominant effect being particle size (Kelvin effect) instead of solute composition (Raoult effect) on the S_c. This is because saturation is inversely proportional to D_p^3 for the Raoult term in equation (1). Even though this is the case, it is still essential to consider the effect of solubility of OC in a mixed particle, which can be important when calculating CCN at a certain size.

Before calculating the CCN concentrations, the values of S_c were determined for the assumptions of OC being equivalent to 3 different acids. As seen in Figure 2, pure oxalic acid required the lowest S_c for activation, even though it has a lower solubility than pure glutaric acid. Even the Type 1 mixed particle type requires a lower S_c than pure glutaric acid. This is a result of the higher density of oxalic acid, which would decrease the S_c according to equation (1). Pure (and mixed) pinonic acid requires a much higher S_c than the other acids because it is not very dense and is practically insoluble, which is why its curve in Figure 2 is close to that of pure EC. The physical properties for the acids differ greatly and have a large impact on S_c, therefore inducing large impacts on the CCN concentration. In Figure 4, the concentrations of CCN were modeled based on the different values of S_c. These results agree with Figure 3 by showing Type 3 as requiring a high S_c close to that of pure EC, and pure oxalic acid requiring the lowest S_c. The Type 3 and pure pinonic acid curves are not smooth, potentially because pinonic acid may be considered only partially soluble. Ervens et al. (2005) observed that solubility was shown to reduce drop concentrations significantly for values less than 0.025 g mL^{-1}.

Overall, in Figure 4 the mixed particles are shifted to the right of the pure acids, suggesting that an addition of 46% insoluble component at 550 nm has a large impact on the CCN concentration. These calculations also show the importance of the OC parameter due to the spread in CCN when considering the different types.

5. Conclusions

The S_c and CCN were calculated for ambient measurements of mixed OC and EC particles observed in Riverside, California, using a Köhler theory model. It was predicted that the soluble OC component would have a large impact on S_c and therefore CCN, however, the Kelvin effect played a larger role in determining these parameters. Sensitivity analysis was done on the assumptions for OC physical characteristics by using density, solubility, and molecular weight of 3 organic acids that have been observed in the atmosphere and are assumed to be representative of the OC fraction. Even though size influenced the S_c more than soluble fraction, what was chosen for the physical characteristics of the soluble component at a constant size did greatly impact the S_c that controlled CCN. Thus, carbonaceous particles with soluble fractions of OC can impact S_c and CCN concentrations, and hence the formation of cloud droplets. However, the large range of S_c from the different physical characteristics used for OC illustrates the need for improved speciation of OC in determining CCN properties.

References

Cruz, C. N., and Pandis, S. N. (2000).Deliquescence and Hygroscopic Growth of Mixed Inorganic-Organic Atmospheric Aerosol, *Environ Sci Technol*, *34* (20), 4313-4319.

Cubison, M. J., Ervens, B., Feingold, G., Docherty, K. S., Ulbrich, I. M., Shields, L., Prather, K., Hering, S., and Jimenez, J. L. (2008).The Influence of Chemical Composition and Mixing State of Los Angeles Urban Aerosol on Ccn Number and Cloud Properties, *Atmos Chem Phys*, *8* (18), 5649-5667.

Dusek, U., Reischl, G. P., and Hitzenberger, R. (2006).Ccn Activation of Pure and Coated Carbon Black Particles, *Environ Sci Technol*, *40* (4), 1223-1230.

Ervens, B., Feingold, G., and Kreidenweis, S. M. (2005). The influence of water-soluble organic carbon on cloud drop number concentration, *J. Geophys. Res.*, *110*, D18211, doi:10.1029/2004JD005634.

Gard, E., Mayer, J. E., Morrical, B. D., Dienes, T., Fergenson, D. P., and Prather, K. A. (1997).Real-Time Analysis of Individual Atmospheric Aerosol Particles: Design and Performance of a Portable Atofms, *Anal Chem*, *69* (20), 4083-4091.

Grosjean, D., and Friedlander, S. K. (1975).Gas-Particle Distribution Factors for Organic and Other Pollutants in Los-Angeles Atmosphere, *Japca J Air Waste Ma*, *25* (10), 1038-1044.

Koch, D. (2001).Transport and Direct Radiative Forcing of Carbonaceous and Sulfate Aerosols in the Giss Gcm, *J Geophys Res-Atmos*, *106* (D17), 20311-20332.

Kohler, H. (1936).The Nucleus in and the Growth of Hygroscopic Droplets., *T Faraday Soc*, *32* (2), 1152-1161.

Kuwata, M., Kondo, Y., Miyazaki, Y., Komazaki, Y., Kim, J. H., Yum, S. S., Tanimoto, H., and Matsueda, H. (2008).Cloud Condensation Nuclei Activity at Jeju Island, Korea in Spring 2005, *Atmos Chem Phys*, *8* (11), 2933-2948.

Novakov, T., and Penner, J. E. (1993).Large Contribution of Organic Aerosols to Cloud-Condensation-Nuclei Concentrations, *Nature*, *365* (6449), 823-826.

Qin, X. Y., Shields, L. G., Toner, S. M., Prather, K. A. (*In preparation.*).A Seasonal Comparison of the Single Particle Mixing State in Riverside, Ca During the Soar 2005 Campaign.

Roberts, G. C., Artaxo, P., Zhou, J. C., Swietlicki, E., and Andreae, M. O. (2002).Sensitivity of Ccn Spectra on Chemical and Physical Properties of Aerosol: A Case Study from the Amazon Basin, *J Geophys Res-Atmos*, *107* (D20), -.

Solomon, S., D. Qin, M. Manning, Z. Chen, M., and Marquis, K. A., M. Tignor, and H. Miller (2007). Climate Change 2007: The Physical Science Basis. Contribution of Working Group I to the Fourth Assessment Report of the Intergovernmental Panel on Climate Change., Cambridge University Press, Cambridge, United Kingdomand New York, NY, USA.

Spencer, M. T., and Prather, K. A. (2006).Using Atofms to Determine Oc/Ec Mass Fractions in Particles, *Aerosol Sci Tech*, *40* (8), 585-594.

Yokouchi, Y., and Ambe, Y. (1985).Aerosols Formed from the Chemical-Reaction of Monoterpenes and Ozone, *Atmos Environ*, *19* (8), 1271-1276.